Pure Appl. Chem., Vol. 85, No. 1, pp. 27–40, 2013.
http://dx.doi.org/10.1351/PAC-CON-12-05-09

A first-principles theoretical study of hydrogen-bond dynamics and vibrational spectral diffusion in aqueous ionic solution: Water in the hydration shell of a fluoride ion*

Jyoti Roy Choudhuri, Vivek K. Yadav, Anwesa Karmakar, Bhabani S. Mallik†, and Amalendu Chandra‡

Department of Chemistry, Indian Institute of Technology, Kanpur 208016, India

Abstract: We present a first-principles simulation study of vibrational spectral diffusion and hydrogen-bond dynamics in solution of a fluoride ion in deuterated water. The present calculations are based on ab initio molecular dynamics simulation for trajectory generation and wavelet analysis for calculations of frequency fluctuations. The O–D bonds of deuterated water in the anion hydration shell are found to have lower stretching frequency than the bulk water. The dynamical calculations of vibrational spectral diffusion for hydration shell water molecules reveal three time scales: a short-time relaxation (~100 fs) corresponding to the dynamics of intact ion-water hydrogen bonds, a slower relaxation (~7.5 ps) corresponding to the lifetimes of fluoride ion-water hydrogen bonds, and an even longer time scale (~26 ps) associated with the escape dynamics of water from the anion hydration shell. However, the slowest time scale is not observed when the vibrational spectral diffusion is calculated over O–D bonds of all water molecules, including those in the bulk.

Keywords: fluoride ions; hydrogen bonds; ionic solution; spectral diffusion.

INTRODUCTION

Understanding the microscopic dynamics of water molecules in ion solvation shells has long been of major interest. In recent years, there have been a number of experimental studies on the dynamics of aqueous solutions using the technique of time-dependent vibrational spectroscopy [1–7]. These studies have looked at the dynamics of so-called vibrational spectral diffusion, which is then mapped to the dynamics of hydrogen bonds in these systems. Experimental studies have also been carried out on the changes of electronic structure of water molecules [8,9] and molecular organization of water [10,11] in ion hydration shells. On the theoretical side, there have been studies in recent years on the vibrational spectral diffusion of hydration shell water molecules in aqueous solutions using a combination of classical dynamics and perturbative method [12] and also by ab initio molecular dynamics [13] simulations. It was shown that the slow escape dynamics of water molecules from ion hydration shells can show up as a long-time component of the spectral dynamics of hydration shell water in dilute solutions.

In this work, we present a detailed dynamical study of water molecules inside the solvation shell of a fluoride ion. Existing microscopic studies on aqueous solutions of fluoride ions are rather limited.

Pure Appl. Chem.* **85, 1–305 (2013). A collection of invited papers based on presentations at the 32nd International Conference on Solution Chemistry (ICSC-32), La Grande Motte, France, 28 August–2 September 2011.

†Present address: Department of Chemistry, Indian Institute of Technology Hyderabad, Yeddumailaram 502205 Andhra Pradesh, India

‡Corresponding author: E-mail: amalen@iitk.ac.in

The structure of water and the nature of ionic hydration have been explored in aqueous solutions of potassium fluoride over a range of concentrations using the neutron diffraction technique [14]. The study reveals that the water structure in the first hydration shell is strongly perturbed but changes outside the hydration shell are rather mild. Vibrational spectroscopy and also vibrational relaxation of water in aqueous solutions of potassium fluoride have also been studied [15,16]. There are theoretical studies in the literature that have looked at the coordination number and radial distribution of water molecules around the fluoride using empirical force fields [17–19] and quantum-mechanical/empirical force fields (QM/MM) [20–22]. Classical molecular dynamics studies of ion-water systems reported very slow dynamics for water around fluoride ion [23]. The dynamical studies regarding self-diffusion and rotational correlation time of the solvation shell water molecules [24] have also been carried out [17,24]. These studies also looked at the residence dynamics of the first solvation shell water molecules around fluoride ion and provide an estimate in the range of 20–30 ps. Molecular dynamics study using density functional theory also reported structural and dynamical properties on water in the first solvation shell [26]. Other dynamical aspects such as dynamics of vibrational frequency fluctuations, so-called vibrational spectral diffusion, and their relations to hydrogen-bond dynamics have not yet been properly addressed for water around fluoride ions. In this paper, such a study of vibrational spectral diffusion and hydrogen-bond dynamics in an aqueous solution containing a fluoride ion is presented from first principles.

The present study is based on ab initio molecular dynamics simulation [27,28] for trajectory generation and wavelet analysis [29–31] for frequency calculation, without involving any empirical potential models. Firstly, the equilibrium aspects of frequency–structure correlations of water in the anionic hydration shell are investigated. We focus on the relations between the stretch frequencies of hydration shell O–D bonds of deuterated water and ion-water hydrogen-bond distance and also on the distribution of hydration shell O–D stretch frequencies as compared to that of bulk water. Next, the hydrogen-bond and residence dynamics of hydration shell and bulk water molecules are calculated through population time correlation function approach and their relations to the dynamics of frequency time correlation and hole dynamics are established.

DETAILS OF SIMULATIONS AND FREQUENCY CALCULATIONS

The ab initio molecular dynamics simulations are carried out by employing the Car–Parrinello method [27,28] and CPMD code [32]. The simulation system contains a single fluoride ion immersed in 31 water molecules kept in a cubic box. The length of the box is determined from the experimental density of NaF in H_2O at 300 K [33]. The box length is calculated assuming the solution consisting of 1 F^- and 1 Na^+ and 30 water, and the Na^+ ion was then replaced by a water molecule. Periodic boundary conditions were implemented in all three dimensions. The electronic structure of the extended system was represented by the Kohn–Sham (KS) formulation [34] of density functional theory within a plane wave basis. The core electrons were treated via the atomic pseudopotentials of Troullier–Martins [35], and the plane wave expansion of the KS orbitals was truncated at a kinetic energy cut-off of 80 Ry. A fictitious mass of $\mu = 800$ a.u. was assigned to the electronic degrees of freedom, and the coupled equations of motion describing the system dynamics was integrated by using a time step of 5 a.u., which is equal to about 0.12 fs.

The hydrogen atoms were assigned the mass of deuterium, to reduce the influence of quantum effects on the dynamical properties. This choice of deuterium mass also ensured that the electronic adiabaticity and the energy conservation were maintained throughout the simulations for chosen values of the fictitious electronic mass parameter and time step. We used the BLYP [36] functional in the present simulations as was also done in many previous simulations of water, aqueous solutions, and other hydrogen-bonded liquids [13,37–56]. The initial configurations of the ion and water molecules were generated by carrying out a classical molecular dynamics simulation using the empirical multisite potential [19,57,58]. Then we equilibrated the system through ab initio molecular dynamics for 10 ps

in a canonical ensemble at 300 K, and thereafter, we continued the run in the microcanonical ensemble for another 50 ps for calculations of various equilibrium and dynamical quantities.

In an aqueous solution of deuterated water, vibration frequencies of O–D bonds fluctuate due to dynamical changes in the local environment. The calculations of such fluctuating frequencies with time are carried out through a time series analysis of the ab initio molecular dynamics trajectories using the wavelet method [29]. In this method, a time-dependent function $f(t)$ is expressed in terms of the basis function, which are constructed as translations and dilations of a mother wavelet ψ.

$$\psi_{a,b}(t) = a^{-1/2}\psi\left(\frac{t-b}{a}\right) \tag{1}$$

and the coefficients of the expansion are given by the wavelet transform of $f(t)$, which is defined as

$$L_\psi f(a,b) = a^{-1/2}\int_{-\infty}^{\infty} f(t)\overline{\psi}\left(\frac{t-b}{a}\right)dt \tag{2}$$

For $a > 0$ and b real. Following our previous work [13], we have used the Morlet–Grossman wavelet [59] as the mother wavelet

$$\psi(t)\frac{1}{\sigma\sqrt{2\pi}}e^{2\pi i\lambda t}e^{-t^2/2\sigma^2} \tag{3}$$

with $\lambda = 1$ and $\sigma = 2$. The wavelet transform of eq. 2 produces a complex surface as a function of the variables a and b. The inverse of the scale factor a is proportional to the frequency and thus the wavelet transform at each b gives the frequency content of $f(t)$ over a time window about b. Following our recent work on aqueous ionic solution [13], the time-dependent function $f(t)$ for a given O–D bond is constructed to be a complex function with its real and imaginary parts, corresponding to the instantaneous O–D distance and the corresponding momentum along the O–D bond and the stretch frequency at a given time $t = b$ is then determined from the scale a that maximizes the modulus of the corresponding wavelet transform at b. The process is then repeated for the entire trajectories and for all the O–D bonds that are there in the solution.

VIBRATIONAL FREQUENCIES OF WATER: HYDRATION SHELL VS. BULK MOLECULES

A water molecule is taken to be in the solvation shell of F^- when its O···F distance is less than 3.4 Å, and it is taken to be hydrogen-bonded if the D···F distance is less than 2.5 Å. Similar cut-offs are also used for oxygen–oxygen and oxygen–hydrogen distances to identify water–water hydrogen bonds. These distances correspond to the first minimum of the intermolecular D···F and O···F (D···O and O···O for water–water pairs) radial distribution functions (results shown in Fig. 1). In Fig. 2, the variation of instantaneous frequency of an O–D mode of a water molecule is shown. The figure shows that there is an increase in frequency about 200 cm^{-1} when the molecule goes out of the solvation shell. The average frequencies of the hydration shell ($\bar{\omega}_{hyd}$) and bulk ($\bar{\omega}_b$) O–D groups are found to be 2322 and 2370 cm^{-1}, respectively. So the individual frequency shifts can be quite different from the average value. Figure 3 shows the power spectrum of the velocity time correlation of the D atoms of hydration shell water molecules. The corresponding results of the bulk water molecules are also shown for comparison. The present result of the red shift of 48 cm^{-1} in the stretch frequency of hydrated O–D bonds is in good agreement with earlier studies [26].

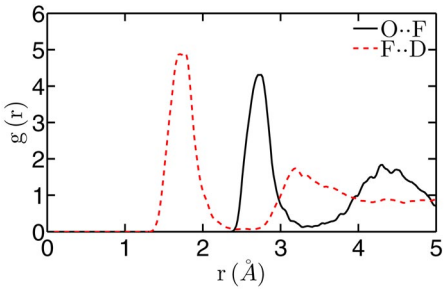

Fig. 1 The radial distribution functions between F^- and water (D_2O). The solid and dashed curves are for F···O and F···D correlations.

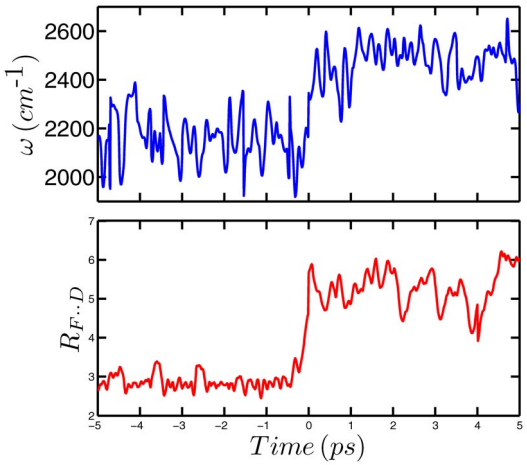

Fig. 2 The time dependence of the fluctuating frequency of an O–D bond of a heavy water as it escapes from the solvation shell of F^- to which it was hydrogen-bonded initially. The time when the escape occurs, i.e., when F···O distance exceeds 3.4 Å, is taken to be $t = 0$, and the frequency and distance fluctuations are shown for 5 ps before and after the escape event. The upper and lower panels show, respectively, the time dependence of the frequency of the O–D bond and the corresponding F···O distance in Å.

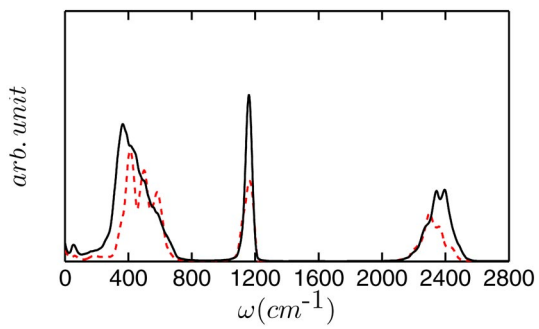

Fig. 3 The power spectrum of the velocity time correlation of deuterium atoms of heavy water in the F^- hydration shell (dashed) and in the bulk region (solid).

Now a detailed analysis has been made regarding the variation of frequency distribution with respect to hydrogen-bond distance and angle. Figure 4a shows the distributions for different hydrogen-bonding environments. Generally, the distributions are found to be rather wide due to inhomogeneous broadening. In Fig. 4b, the frequency distributions are shown for different hydrogen-bond angles. It is seen that the rotational effects can alter the strength of hydrogen bonds, which in turn can alter the vibrational frequencies for both hydration shell and bulk modes. In Fig. 5a, we have presented a detailed

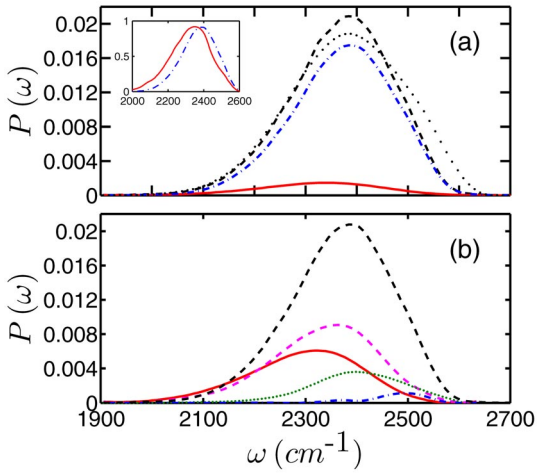

Fig. 4 (a) The distribution of O–D stretch frequencies averaged over all O–D modes (dashed), those in the bulk (dashed–dotted), and those in the F^- hydration shell (solid). The dotted curve shows the corresponding distribution for pure water. The inset shows the frequency distributions of bulk and hydration shell O–D bonds each normalized to the maximum value of 1. (b) The frequency distributions for different values of the hydrogen-bond angle ϕ. The solid, dashed, dotted, and dashed–dotted curves are for O–D groups with hydrogen-bond angles of 5 ± 5°, 15 ± 5°, 25 ± 5°, and 35 ± 5°, respectively. The dashed curve with higher intensity represents averages over all O–D groups.

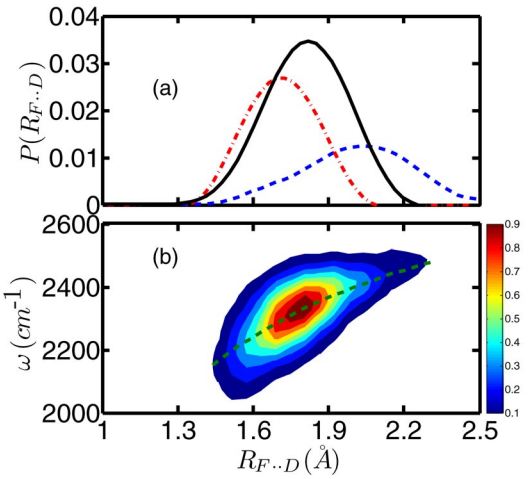

Fig. 5 (a) The distribution of the F···D distance for fixed values of the O–D frequency. The solid, dashed-dotted and dashed curves are for O–D frequency $\Delta\omega = 0 \pm 5$ cm^{-1}, -100 ± 5 cm^{-1}, and 100 ± 5 cm^{-1}, respectively, where $\Delta\omega$ represents the deviation from the average frequency. (b) Joint probability distribution of the O–D frequency and F···D distance. The results are for deuterated water molecules in the F^- hydration shell.

analysis of the distribution of D···F distance for three fixed values of O–D frequency (within ±5 cm^{-1}). It is seen that the corresponding distributions shift toward larger values with increase in frequency. However, fairly wide distributions with significant overlaps are also observed, which means a single instantaneous frequency cannot be assigned to a given D···F distance. However, such a one-to-one frequency–structure correlation seems to be present on average. This is shown more clearly in Fig. 5b through the contour plots of the conditional probability distributions of observing a particular frequency for a given D···F distance. Clearly, the substantial width in the probability distributions rules out the possibility of assigning a single instantaneous frequency to a given D···F distance. On average, however, the frequency is seen to be a monotonic function of the D···F distance as shown by the dashed line in Fig. 5b. This means a frequency–structure correlation is present on average in the ion hydration shell where the frequency of an O–D bond decreases with decrease of the associated D···F hydrogen-bond distance.

DYNAMICS OF HYDROGEN BONDS AND ESCAPE OF WATER FROM ION HYDRATION SHELL

The dynamics of ion-water hydrogen bonds is investigated by using the so-called population correlation function approach [13,60–68]. In this approach, we define two hydrogen-bond population variables: $h(t)$ and $H(t)$, where $h(t)$ is unity when a particular F^--water pair is hydrogen-bonded at time t and zero otherwise. $H(t) = 1$ if the ion-water pair remains continuously hydrogen-bonded from $t = 0$ to time t and it is zero otherwise. We calculate the continuous hydrogen-bond time correlation function $S_{HB}(t)$, which is defined as [60–63,66–68]

$$S_{HB}(t) = \frac{\langle h(0)H(t)\rangle}{\langle h(0)^2\rangle} \tag{4}$$

where < ... > denotes an average over all ion-water pairs. $S_{HB}(t)$ describes the probability that an initially hydrogen-bonded ion-water pair remains bonded at all times up to t. The associated integrated relaxation time τ_{HB} gives the average lifetime of a hydrogen bond between F^- and a water molecule in its hydration shell. The intermittent correlation function is defined as [60–68]

$$C_{HB}(t) = \frac{\langle h(0)h(t)\rangle}{\langle h(0)^2\rangle} \tag{5}$$

$C_{HB}(t)$ describes the probability that an ion-water hydrogen bond is intact at time t, given that it was intact at time $t = 0$, independent of possible breaking in the interim time. After a hydrogen bond between the F^- ion and water is broken, the water-ion can remain as nearest neighbors for some time before either reformation of hydrogen bond occurs or the molecules diffuse away from each other. We also calculate a third probability function $N_{HB}(t)$, which describes the time-dependent probability that an ion-water hydrogen bond is broken at time zero, but the two species remain in the vicinity of each other, i.e., as nearest neighbors, but not hydrogen-bonded at time t. Following previous work [64], a simple rate equation for the reactive flux is written in terms of $C_{HB}(t)$ and $N_{HB}(t)$

$$\frac{-dC_{HB}(t)}{dt} = k_{HB}C_{HB}(t) - k'_{HB}N_{HB}(t) \tag{6}$$

where k_{HB} and k'_{HB} are the forward and backward rate constants for hydrogen-bond breaking. The inverse of k_{HB} corresponds to the average lifetime of an ion-water hydrogen bond and can be correlated with τ_{HB} obtained from the route of continuous hydrogen-bond time correlation function.

The results of the continuous and intermittent correlation functions for ion-water hydrogen bonds are shown in Fig. 6a, and the corresponding lifetimes are included in Table 1. Integration of $S_{HB}(t)$ yields a value of 7.65 ps for τ_{HB}. This ion-water hydrogen-bond lifetime is longer than the lifetimes of hydrogen bonds in pure water, which was found to be ~2 ps [66]. We have used a least-squares fit of the simulation results of $C_{HB}(t)$ and $N_{HB}(t)$ to eq. 6 to obtain the ion-water hydrogen-bond lifetimes from the route of intermittent correlations. We performed the fitting in the short-time region $0 < t < 8$ ps to obtain the rate constants for the short-time part of the relaxation, and we also carried out the fitting on the longer time region $8 < t < 30$ ps to calculate these quantities for the slower, long-time part of the relaxation. The inverses of the corresponding forward rate constants, which correspond to the average hydrogen-bond lifetimes, are denoted as $1/k_{HB;short}$ and $1/k_{HB;long}$, and their values are found to be 7.27 and 20.83 ps, respectively. We note that the values of $1/k_{HB;short}$ are similar to τ_{HB} obtained from the route of continuous correlation functions because both $S_{HB}(t)$ and the short-time part of the reactive flux capture the hydrogen-bond-breaking dynamics due to librational, rotational, and short-time translational motion, and, henceforth, this time constant of ~7.27 ps will be referred to as the fluoride ion-water hydrogen-bond lifetime.

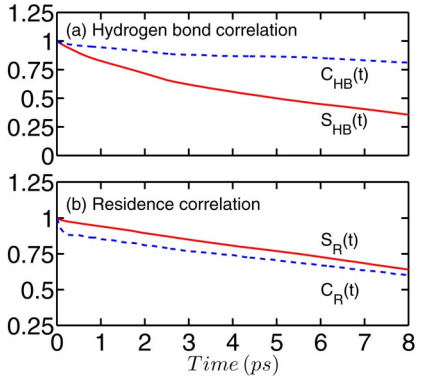

Fig. 6 (a) The time dependence of the continuous (solid) and intermittent (dashed) correlation functions of F^--water hydrogen bonds. (b) The escape dynamics of water molecules from the hydration shell of F^-. The solid and dashed curves are for the continuous (with an allowance time of 2 ps) and intermittent residence time correlation functions of water molecules in the F^- solvation shell.

Table 1 The average lifetime of fluoride ion-water and all hydrogen bonds (HBs) of the solution. The residence time of water in the ion hydration shell is also included. All time constants are expressed in ps.

Quantity	Ion-water HBs	All HBs
τ_{HB}	7.65	3.87
$1/k_{HB:short}$	7.27	3.20
$1/k_{HB:long}$	20.83	20.64
τ_R	26.05	–

The residence times of water molecules in the ion hydration shell are calculated by following a similar population correlation function approach [13]. Two residence variables $g(t)$ and $g'(t;t^*)$ are defined where $g(t)$ is unity if the F^--oxygen distance of the ion-water pair is less than 3.4 Å at time t (i.e., the water is in the hydration shell of F^-) and it is zero otherwise, whereas the variable $g'(t;t^*)$ is

one when a water molecule remains continuously in the same hydration shell up to time t from $t = 0$, subject to an allowance time t^* and it is zero otherwise. The correlation functions [23] are constructed as

$$S_R(t) = \langle g(0)g'(t;t^*)\rangle / \langle g(0)^2\rangle \tag{7}$$

$$C_R(t) = \langle g(0)g(t)\rangle / \langle g(0)^2\rangle \tag{8}$$

where $S_R(t)$ describes the probability that a water molecule, which was in the hydration shell of the ion at time $t = 0$, remains continuously in the hydration shell up to time t subject to the allowance time t^* and the associated relaxation time, which we call the residence time, is denoted as τ_R. Thus, if the water molecule leaves the hydration shell for a period less than t^* between the time 0 and t, it is assumed to have not left the hydration shell at all. The intermittent residence correlation function $C_R(t)$ gives the probability that a water molecule, which was in the hydration shell of an ion at the initial time, is also found to be in the same hydration shell at time t irrespective of what has happened in the interim period. In Fig. 6b, we have shown the decay of $S_R(t)$ and $C_R(t)$. The calculation of residence time τ_R has been done by explicit integration of $S_R(t)$ from simulations until 10 ps and by calculating the integral for the tail part from fitted exponential functions. Following previous work [23,25], we took the allowance time to be 2 ps for the continuous residence function and found a value of 26.05 ps for the residence time of water molecules in the F^- solvation shell. We also extracted the residence time from the intermittent correlation by following the method of ref. [23], and a very similar value is found. Thus, from the similarity of the time scales, we can conclude that the longer time scale of $1/k_{HB;long}$ actually corresponds to the residence time of a water molecule in the hydration shell of a tagged water to which it was hydrogen-bonded at time $t = 0$. Hence, this longer time scale actually corresponds to the escape dynamics or slow diffusion of a water molecule from the hydration shell of the fluoride ion.

VIBRATIONAL SPECTRAL DIFFUSION OF HYDRATION SHELL WATER MOLECULES

In this section, we carry out hole dynamics [12,13,66,69] calculations of O–D stretch modes of water in F^- hydration shell. It is assumed that at time $t = 0$, a hole of the following Gaussian form is created in the ground-state frequency distribution

$$P_h(\omega,0) = P_{eq}e^{-(\omega-\omega_p)^2/2\sigma^2} \tag{9}$$

where ω_p is the pulse center frequency and $P_{eq}(\omega)$ denotes the equilibrium frequency distribution of the O–D modes of interest. Clearly, the initial distribution of the remaining O–D frequencies $P_r(\omega,0)$, i.e., the ones remaining in the ground state in experimental situations, is equal to $P_{eq}(\omega) - P_h(\omega,0)$. We use a Gaussian pulse of full width (2σ) 140 cm^{-1} and calculate the time evolution of the nonequilibrium distributions $P_r(\omega,t)$ and $P_h(\omega,t)$ from a large set of system trajectories reflecting the initial distributions $P_r(\omega,0)$ and $P_h(\omega,0)$, respectively. The average frequency of the hole modes at time t is then calculated from the following relation [12,13,66,69]

$$\bar{\omega}_h(t) = \frac{1}{N_h}\int d\omega\omega P_h(\omega,t) \tag{10}$$

where $N_h = \int d\omega P_h(\omega,0)$. The average time-dependent frequency of the remaining modes is calculated in a similar way by using the remaining distribution in eq. 10.

Firstly, the hole dynamics calculations are carried out on a subset of hydration shell O–D stretch modes. The holes are created in two different frequency regions: one centered in the red side at $\omega_p = \bar{\omega}_{hyd} - 100$ cm^{-1} and the other centered in the blue side at $\omega_p = \bar{\omega}_{hyd} + 100$ cm^{-1} where, as defined earlier, $\bar{\omega}_{hyd}$ is the average frequency of all the O–D groups that are in the hydration shell of the F^- ion. The dynamics of the average frequency shifts of the hole and remaining modes of hydration shell water

molecules are observed. A Metropolis Monte Carlo-like algorithm [70] is employed to effect the creation of a chosen hole, red or blue so as to satisfy the distribution of eq. 9. In this approach, we first choose an O–D group of frequency ω_i in the hydration shell at a given time step along the trajectory to include this mode as a hole mode. The value of the corresponding Gaussian probability $P_i = e^{-(\omega_i - \omega_p)^2/2\sigma^2}$. After that, a random number y_i from a uniform distribution between 0 and 1 is generated and if y_i comes out to be less than the Gaussian probability P_i, the chosen mode ω_i is included as a hole mode. The above exercise is repeated for all the O–D groups in the F^- hydration shell and over many different initial times to ensure that, on average, the hole modes satisfy the distribution of eq. 9.

We investigated the time evolution of the average frequencies of the hole and remaining modes in the hydration shell after the hole is created at $t = 0$. In Fig. 7, we have shown the average frequencies of the hole modes ($\Delta\bar{\omega}_h$) for both blue and red excitations, and the corresponding results for the remaining modes ($\Delta\bar{\omega}_r$) are shown in Fig. 8. Here, the frequency is expressed in terms of the shift ($\Delta\omega$) from the equilibrium value averaged over all the modes. We observe a fast decay and an oscillation at short times followed by slower decay extending to a few ps. We used the following function including a damped oscillatory function to fit the calculated results of spectral diffusion [13,66,69]

$$f(t) = a_0 \cos\omega_s t e^{-t/\tau_0} + a_1 e^{-t/\tau_1} + \left(1 - a_0 - a_1\right)^{-t/\tau_2} \tag{11}$$

The details of the fitting parameters including the weights are included in Table 2. To verify the origin of this oscillation, a separate calculation of the power spectrum of the relative velocity of an initially hydrogen-bonded O···F pair have been carried out (results not shown). In the power spectrum, due to intermolecular bending and stretching vibrations of the hydrogen-bonded F^--water pair, enhanced intensities are found at around 50 and 180 cm^{-1}. Both bending and stretching modes of intermolecular vibrations can modulate the O–D stretch frequencies and hence contribute to the short-time oscillation

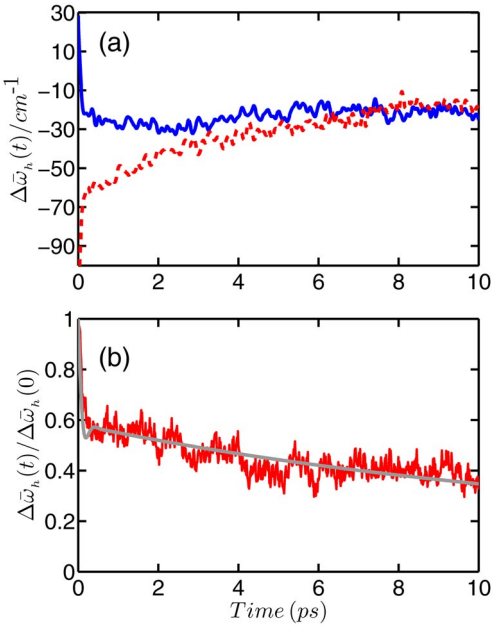

Fig. 7 The time variation of the (a) average frequency shifts of the hole modes after excitations in the higher- and lower-frequency regions of the hydration shell O–D modes. The corresponding results for the excitation in the lower-frequency side after normalization by the initial frequency shift are shown in (b). The solid and dashed curves correspond to excitations in the higher and lower frequencies, respectively. The smooth solid curve in (b) represents the fit by a function of eq. 11.

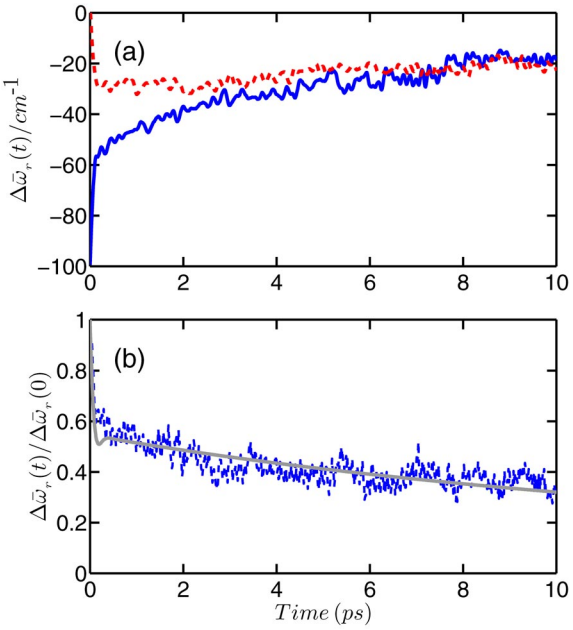

Fig. 8 The time variation of the (a) average frequency shifts of the remaining modes after hole creation in the higher- and lower-frequency regions of the hydration shell O–D modes. The corresponding results for the excitation in the higher-frequency side after normalization by the initial frequency shift are shown in (b). As in the previous figure, the solid and dashed curves correspond to excitations in the higher and lower frequencies, respectively. The smooth solid curve in (b) represents the fit by a function of eq. 11.

Table 2 The results of the time scales of vibrational spectral diffusion for the hydration shell O–D stretch modes. The time constants (ps), frequency (cm^{-1}) and weights of time-dependent frequency shifts of hole and remaining modes for red and blue excitations of O–D bonds in the F^- hydration shell.

Quantity	Excitation	τ_0	τ_1	τ_2	ω_s	a_0	a_1
$\Delta\bar{\omega}_h(t)$	red	0.09	7.95	28.58	65.53	0.42	0.15
$\Delta\bar{\omega}_r(t)$	blue	0.08	7.25	25.52	63.49	0.45	0.11

of the hole dynamics. It is also clear from the results of the previous section that the two slower relaxation times of spectral diffusion, τ_2 and τ_3 of Table 2, correspond to the lifetimes of ion-water hydrogen bonds and the residence time of water in the ion hydration shell, respectively.

The results of vibrational spectral diffusion discussed above are for the O–D stretch modes of water molecules in the F^- hydration shell only. In addition, we have also investigated the dynamical response of all the O–D modes in the solution. The calculation of the average frequency shift of the hole and remaining modes for both red and blue excitations are shown in Figs. 9 and 10, and the corresponding time constants and weights are included in Table 3. The results of our hydrogen-bond dynamics calculations for all O–D modes are included in Table 1. These calculations reveal that the decay is faster as compared to hydration shell O–D modes. In particular, the slowest component corresponding to the escape dynamics of water from ion solvation shell is not found to be present here. This is likely due to the very small fraction of such hydration shell O–D modes with respect to all the O–D modes that are present in the current simulation system.

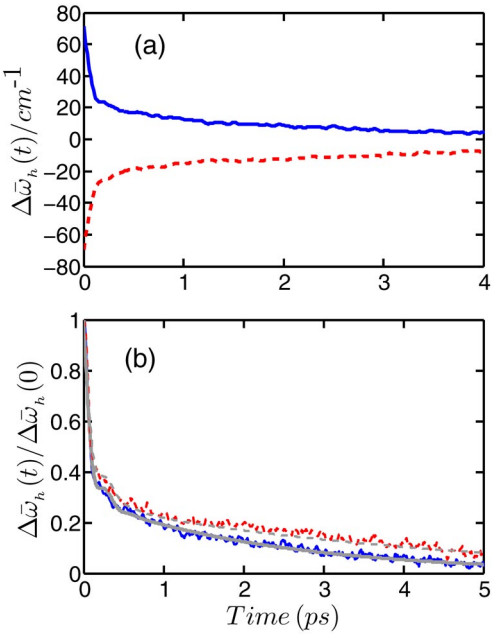

Fig. 9 The time variation of the (a) average frequency shifts of the hole modes when all O–D modes are considered in the calculations. The corresponding results after normalization by the initial frequency shifts are shown in (b). As before, the solid and dashed curves correspond to excitations in the higher and lower frequencies, respectively. The smooth solid curves in (b) represent the fits by a function of eq. 11.

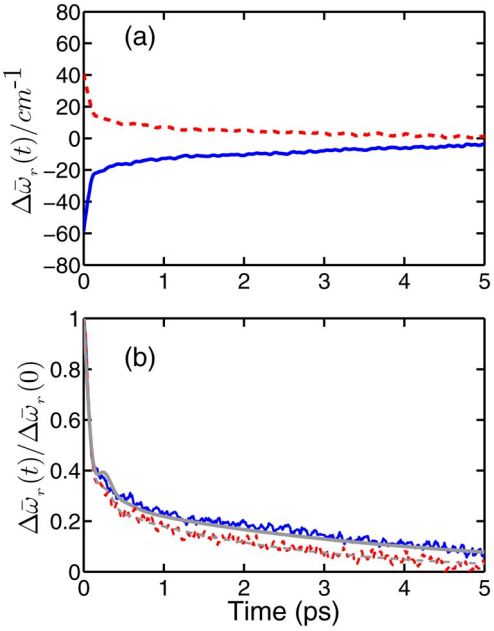

Fig. 10 The time variation of the (a) average frequency shifts of the remaining modes when all O–D modes are considered in the calculations. The corresponding results after normalization by the initial frequency shifts are shown in (b). The solid and dashed curves correspond to excitations in the higher and lower frequencies, respectively. The smooth solid curves in (b) represent the fits by a function of eq. 11.

Table 3 The results of the spectral diffusion for all O–D modes. The units of different quantities are as in Table 2.

Quantity	Excitation	τ_0	τ_1	τ_2	ω_s	a_0	a_1
$\Delta\bar{\omega}_h(t)$	blue	0.13	0.12	2.34	99.1	0.21	0.48
$\Delta\bar{\omega}_r(t)$	blue	0.11	0.20	3.9	100.33	0.29	0.42
$\Delta\bar{\omega}_h(t)$	red	0.12	0.19	4.12	91.41	0.24	0.47
$\Delta\bar{\omega}_r(t)$	red	0.15	0.13	2.3	95.89	0.17	0.55
$C\omega(t)$	–	0.12	0.18	3.4	117.96	0.28	0.45

SUMMARY AND CONCLUSIONS

We have presented a theoretical study of hydrogen-bond dynamics and vibrational spectral diffusion in an aqueous ionic solution containing a fluoride ion from first-principles simulations without employing any empirical potential models. The method of ab initio molecular dynamics has been used for trajectory generation, and the wavelet analysis has been employed for frequency calculations. First, the equilibrium properties regarding the frequency–structure correlations of water molecules in the F^- hydration shell are looked at. It is found that the O–D bonds in the hydration shell of F^- ion, i.e., hydrogen-bonded to the fluoride ion, have lower stretching frequency than those in bulk water. On average, the frequencies of hydration shell O–D modes are found to increase with the increase of the ion-water hydrogen-bond distance. The stretching frequency of O–D modes is also found to change with changes in the hydrogen-bond angle.

On the dynamical side, it is found that fluoride ion-water hydrogen bonds have much longer lifetime than water–water hydrogen bonds. The study of hole-burning dynamics reveals three time scales: a short time relaxation of ~100 fs corresponding to the dynamics of intact ion-water hydrogen bonds, a slower relaxation with a time scale of ~7.5 ps corresponding to the ion-water hydrogen-bond lifetime, and another longer time constant of ~26 ps corresponding to the escape dynamics of water from the fluoride ion hydration shell. These three time scales in the spectral diffusion of water in the hydration shell in the dilute solution is in line with the earlier work for water near a halide ion [12,13]. However, the longest time scale is found to be absent when the spectral diffusion was calculated by averaging over all the water molecules. This is likely due to the small weight that the hydration shell water molecules make to the overall dynamical behavior of all water molecules in the aqueous system considered in the present study. In the present work, we have considered an aqueous solution containing a single fluoride ion. It would be interesting to study the dynamical properties for higher concentration of fluoride ions and also in the presence of counterions. Work in this direction is in progress.

ACKNOWLEDGMENT

Financial support from the Department of Science and Technology (DST) and Council of Scientific and Industrial Research (CSIR), Government of India, is gratefully acknowledged.

REFERENCES

1. S. Woutersen, H. J. Bakker. *Phys. Rev. Lett*. **96**, 138305 (2006).
2. H.-K. Nienhuys, A. J. Lock, R. A. van Santen, H. J. Bakker. *J. Chem. Phys*. **117**, 8021 (2002).
3. M. Rini, B.-Z. Magnes, E. Pines, E. T. J. Nibbering. *Science* **301**, 349 (2003).
4. H. S. Tan, I. R. Piletic, R. E. Riter, N. E. Levinger, M. D. Fayer. *Phys. Rev. Lett*. **94**, 057405 (2005).
5. M. F. Kropman, H. J. Bakker. *Science* **291**, 2118 (2001).
6. M. F. Kropman, H. J. Bakker. *J. Chem. Phys*. **115**, 8942 (2001).

7. S. Park, M. D. Fayer. *Proc. Natl. Acad. Sci. USA* **104**, 16731 (2007).
8. W. H. Robertson, M. A. Johnson. *Annu. Rev. Phys. Chem*. **54**, 173 (2003).
9. C. D. Cappa, J. D. Smith, K. R. Wilson, B. M. Messer, M. K. Gilles, R. C. Cohen, R. J. Saykally. *J. Phys. Chem. B* **109**, 7046 (2005).
10. R. Leberman, A. K. Soper. *Nature* **378**, 364 (1995).
11. P. H. K. de Jong, G. W. Neilson, M.-C. Bellisent-Funel. *J. Chem. Phys*. **105**, 5155 (1996).
12. B. Nigro, S. Re, D. Laage, R. Rey, J. T. Hynes. *J. Phys. Chem. A* **110**, 11237 (2006).
13. B. S. Mallik, A. Semparithi, A. Chandra. *J. Chem. Phys*. **129**, 194512 (2008).
14. A. K. Soper, K. Weckström. *Biophys. Chem*. **124**, 180 (2006).
15. Z. S. Nickolov, J. D. Miller. *J. Colloid Interface Sci.* **287**, 572 (2005).
16. M. F. Kropman, H. J. Bakker. *Chem. Phys. Lett.* **370**, 741 (2003).
17. S. H. Lee, J. C. Rasaiah. *J. Phys. Chem.* **100**, 1420 (1996).
18. S. S. Xantheas, L. X. Dang. *J. Phys. Chem*. **100**, 3989 (1996).
19. S. Koneshan, J. C. Rasaiah, R. M. Lynden-Bell, S. H. Lee. *J. Phys. Chem. B* **102**, 4193 (1998).
20. A. Ohrn, G. Karlström. *J. Phys. Chem. B* **108**, 8452 (2004).
21. A. Tongraar, B. M. Rode. *Phys. Chem. Chem. Phys.* **5**, 357 (2003).
22. R. Ayala, J. M. Martínez, R. R. Pappalardo, E. S. Marcos. *J. Chem. Phys.* **119**, 9538 (2003).
23. S. Chowdhuri, A. Chandra. *J. Phys. Chem. B* **110**, 9674 (2006).
24. H. Ohtaki, T. Radnai. *Chem. Rev.* **93**, 1157 (1993).
25. R. W. Impey, P. A. Madden, I. R. McDonald. *J. Phys. Chem.* **87**, 5071 (1983).
26. J. M. Heuft, E. J. Meijer. *J. Chem. Phys.* **122**, 094501 (2005).
27. R. Car, M. Parrinello. *Phys. Rev. Lett.* **55**, 2471 (1985).
28. D. Marx, J. Hutter. "Ab initio molecular dynamics: Theory and implementation", in *Modern Methods and Algorithms of Quantum Chemistry*, J. Grotendorst (Ed.), NIC, FZ Jülich (2000).
29. M. Fuentes, P. Guttorp, P. D. Sampson. In *Statistical Methods for Spatio-Temporal Systems*, B. Finkenstädt, L. Held, V. Isham (Eds.), Chap. 3, Chapman & Hall/CRC, Boca Raton (2007).
30. L. V. Vela-Arevalo, S. Wiggins. *Int. J. Bifurcation. Chaos Appl. Sci. Eng.* **11**, 1359 (2001).
31. A. Semparithi, S. Keshavamurthy. *Phys. Chem. Chem. Phys.* **5**, 5051 (2003); see Sect. IV for a calculation of time-dependent frequencies using the wavelet method.
32. J. Hutter, A. Alavi, T. Deutsch, M. Bernasconi, S. Goedecker, D. Marx, M. Tuckerman, M. Parrinello. *CPMD program*, MPI für Festkörperforschung and IBM Zurich Research Laboratory.
33. D. R. Lide (Ed.). *Handbook of Chemistry and Physics*, Vol. 87, CRC, Boca Raton/Taylor & Francis, London (2006).
34. W. Kohn, L. J. Sham. *Phys. Rev.* **140**, A1133 (1965).
35. N. Troullier, J. L. Martins. *Phys. Rev. B* **43**, 1993 (1991).
36. (a) A. D. Becke. *Phys. Rev. A* **38**, 3098 (1988); (b) C. Lee, W. Yang, R. G. Parr. *Phys. Rev. B* **37**, 785 (1988).
37. K. Laasonen, M. Sprik, M. Parrinello, R. Car. *J. Chem. Phys.* **99**, 9080 (1993).
38. M. Sprik, J. Hutter, M. Parrinello. *J. Chem. Phys*. **105**, 1142 (1996).
39. (a) P. L. Silvestrelli, M. Parrinello. *J. Chem. Phys*. **105**, 1142 (1996); (b) P. L. Silvestrelli, M. Parrinello. *Phys. Rev. Lett.* **82**, 3308 (1999); (c) P. L. Silvestrelli, M. Parrinello. *J. Chem. Phys*. **111**, 3572 (1999); (d) P. L. Silvestrelli, M. Bernasconi, M. Parrinello. *Chem. Phys. Lett*. **277**, 478 (1997).
40. (a) M. Krack, A. Gambirasio, M. Parrinello. *J. Chem. Phys.* **117**, 9409 (2002); (b) B. Chen, I. Ivanov, M. L. Klein, M. Parrinello. *Phys. Rev. Lett.* **91**, 215503 (2003).
41. S. Izvekov, G. A. Voth. *J. Chem. Phys.* **116**, 10372 (2002).
42. (a) M. Boero, K. Terakura, T. Ikeshoji, C. C. Liew, M. Parrinello. *Phys. Rev. Lett*. **85**, 3245 (2000); (b) M. Boero, K. Terakura, T. Ikeshoji, C. C. Liew, M. Parrinello. *J. Chem. Phys*. **115**, 2219 (2001).

43. M. Boero. *J. Phys. Chem. A* **111**, 12248 (2007).
44. (a) D. Marx, M. E. Tuckerman, J. Hutter, M. Parrinello. *Nature* (*London*) **397**, 601 (1999); (b) M. E. Tuckerman, D. Marx, M. Parrinello. *Nature* (*London*) **417**, 925 (2002).
45. B. Kirchner, J. Stubbs, D. Marx. *Phys. Rev. Lett*. **89**, 215901 (2002).
46. J. M. Heuft, E. J. Meijer. *Phys. Chem. Chem. Phys*. **8**, 3116 (2006).
47. M. Cavallari, C. Cavazzoni, M. Ferrario. *Mol. Phys*. **102**, 959 (2004).
48. T. Ikeda, M. Hirata, T. Kimura. *J. Chem. Phys*. **119**, 12386 (2003).
49. K. Leung, S. B. Rempe. *J. Am. Chem. Soc.* **126**, 344 (2004).
50. (a) L. M. Ramaniah, M. Barnasconi, M. Parrinello. *J. Chem. Phys.* **111**, 1587 (1999); (b) A. P. Lyubartsev, K. Laasonen, A. Laaksonen. *J. Chem. Phys*. **114**, 3120 (2001).
51. M.-P. Gaigeot, M. Sprik. *J. Phys. Chem. B* **108**, 7458 (2004).
52. E. Tsuchida, Y. Kanada, M. Tsukda. *Chem. Phys. Lett*. **311**, 236 (1999).
53. M. Pagliai, G. Cardini, R. Righini, V. Schettino. *J. Chem. Phys*. **119**, 6655 (2003).
54. J. A. Morrone, M. E. Tuckerman. *J. Chem. Phys.* **117**, 4403 (2002).
55. M. Diraison, G. J. Martyna, M. E. Tuckerman. *J. Chem. Phys*. **111**, 1096 (1999).
56. A. D. Boese, A. Chandra, J. M. L. Martin, D. Marx. *J. Chem. Phys*. **119**, 5965 (2003).
57. H. J. C. Berendsen, J. R. Grigera, T. P. Straatsma. *J. Phys. Chem*. **91**, 6269 (1987).
58. L. X. Dang. *Chem. Phys. Lett.* **200**, 21 (1992).
59. R. Carmona, W. Hwang, B. Torresani. *Practical Time-frequency Analysis: Gabor and Wavelet Transforms with an Implementation*, Academic, New York (1998).
60. D. Rapaport. *Mol. Phys*. **50**, 1151 (1983).
61. A. Chandra. *Phys. Rev. Lett*. **85**, 768 (2000).
62. S. Balasubramanian, S. Pal, B. Bagchi. *Phys. Rev. Lett*. **89**, 115505 (2002).
63. A. Luzar. *J. Chem. Phys*. **113**, 10663 (2000).
64. (a) A. Luzar, D. Chandler. *Phys. Rev. Lett*. **76**, 928 (1996); (b) A. Luzar, D. Chandler. *Nature* (*London*) **379**, 55 (1996).
65. (a) H. Xu, B. J. Berne. *J. Phys. Chem. B* **105**, 11929 (2001); (b) H. Xu, H. A. Stern, B. J. Berne. *J. Phys. Chem. B* **106**, 2054 (2002).
66. B. S. Mallik, A. Semparithi, A. Chandra. *J. Phys. Chem. A* **112**, 5104 (2008).
67. (a) S. Chowdhuri, A. Chandra. *Chem. Phys. Lett.* **373**, 79 (2003); (b) S. Chowdhuri, A. Chandra. *J. Chem. Phys.* **115**, 3732 (2001).
68. M. Jana, S. Bandyopadhyay. *J. Chem. Phys*. **134**, 025103 (2011).
69. (a) R. Rey, K. B. Moller, J. T. Hynes. *J. Phys. Chem. A* **106**, 11993 (2002); (b) K. B. Moller, R. Rey, J. T. Hynes. *J. Phys. Chem. A* **108**, 1275 (2004).
70. M. P. Allen, D. J. Tildesley. *Computer Simulation of Liquids*, Oxford, New York (1987).

